Ecological Indicators 147 (2023) 110000

Contents lists available at ScienceDirect

Ecological Indicators

journal homepage: www.elsevier.com/locate/ecolind

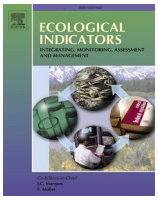

Land surface phenology indicators retrieved across diverse ecosystems using a modified threshold algorithm

Qiaoyun Xie [a,b,*], Caitlin E. Moore [c,d], Jamie Cleverly [e], Christopher C. Hall [a], Yanling Ding [f], Xuanlong Ma [g], Andy Leigh [a], Alfredo Huete [a]

[a] Faculty of Science, University of Technology Sydney, Sydney, NSW 2007, Australia
[b] Department of Environmental Science, Policy and Management, UC Berkeley, Berkeley, CA 94720, USA
[c] School of Agriculture and Environment, The University of Western Australia, Crawley, WA 6010, Australia
[d] Institute for Sustainability, Energy and Environment, University of Illinois Urbana-Champaign, Urbana, IL 61801, USA
[e] Terrestrial Ecosystem Research Network, College of Science and Engineering, James Cook University, Cairns, QLD 4811, Australia
[f] Key Laboratory of Geographical Processes and Ecological Security in Changbai Mountains, Ministry of Education, School of Geographical Sciences, Northeast Normal University, Changchun 130024, China
[g] College of Earth and Environmental Sciences, Lanzhou University, Lanzhou, Gansu 730000, China

ARTICLE INFO

Keywords:
Land surface phenology
Vegetation index
Ecological modelling
Ecosystem dynamics
Climate change
Precision agriculture

ABSTRACT

Land surface phenology (LSP), the study of the seasonal vegetation dynamics from remote sensing imagery, provides crucial information for plant monitoring and reflects the responses of ecosystems to climate change. The Moderate Resolution Imaging Spectroradiometer (MODIS) phenology product (MCD12Q2) provides global LSP information, but it has large spatial gaps in many regions, especially in ecosystems where rainfall influences phenology more than temperature. This study aimed to improve spatial coverage of LSP retrieval in these ecosystems. To do so, we used a regionally modified threshold algorithm for LSP retrievals, which were tested over continental Australia as it includes diverse landscapes of arid, mesic, and forest environments. We generated LSP metrics annually from 2003 to 2018 using satellite Enhanced Vegetation Index (EVI) time series at 500 m resolution, including the start, peak, end, and length of growing seasons, the minimum EVI value prior to and after the peak date, the seasonal maximum EVI value, the integral EVI value during the growing season (an approximation of productivity), and seasonal amplitude (maximum EVI value minus minimum EVI). Our regionally optimised algorithm improved the spatial coverage of LSP information in Australia from only 26 % of the continent to 70 % averaged across 16 years. Our results showed that the growing season amplitude was low (EVI < 0.1) over arid/semi-arid shrublands and savannas, tropical and subtropical savannas, and temperate evergreen forests, whose LSP metrics were captured by our regional algorithm and not by the global product. Some ecosystems, such as arid/semi-arid shrublands and savannas, showed more irregular phenology with low seasonal dynamics, and the growing seasons could skip a year or occur more than once in a year depending on climate conditions. Our algorithm was more sensitive to ecosystems with low seasonal amplitudes. We found that the detectability of LSP increases as the growing season amplitude increases, regardless of vegetation cover. Evaluation of the LSP metrics using eddy covariance flux tower measurements of gross primary productivity (GPP) demonstrated the reliability and accuracy of the algorithm. These improved LSP retrievals provide a greater understanding of the vegetation phenology across diverse ecosystems, especially savanna, shrubland, and evergreen forest ecosystems that cover more than 30 % of the land globally. The LSP provides essential information for ecological and agricultural studies such as quantifying bushfire fuel accumulation and forest carbon cycling, whilst enhancing our capacity for quantifying ecological responses to climate change.

* Corresponding author at: Faculty of Science, University of Technology Sydney, Sydney, NSW 2007, Australia.
E-mail address: Qiaoyun.Xie@uts.edu.au (Q. Xie).

https://doi.org/10.1016/j.ecolind.2023.110000
Received 26 July 2022; Received in revised form 29 December 2022; Accepted 7 February 2023
Available online 13 February 2023

1. Introduction

Vegetation phenology is defined as the occurrence of vegetation life cycle events, including bud break, flowering, or leaf senescence (Henebry and de Beurs, 2013). Phenology dynamics affect the exchange of water, carbon, and energy in ecosystems (White et al., 2009; Puma et al., 2013; Delbart et al., 2015), therefore phenology can provide an indicator of global carbon exchange and the impact of climate change on ecosystems (Myneni et al., 1997; Huete et al., 2006; Linderholm, 2006; Richardson et al., 2013; Xu et al., 2019). Vegetation phenology can also support the observation and modelling of biosphere processes, agricultural management, and detect changes in land cover and land use (Lymburner et al., 2011; Wang et al., 2017). The use of satellite-based observations allows us to apply plot-based plant observations across much larger scales in order to explore land surface phenology (LSP) at the global scale (Helman, 2017). LSP serves as a bio-indicator of ongoing climate change impacts (Ren et al., 2020), and LSP parameters are also important for biosphere models, which need an accurate representation of phenological variation (Richardson et al., 2012). Satellite remote sensing estimates of LSP can also greatly improve estimates of productivity, carbon sequestration, and climate change impacts at large scales (Baldocchi et al., 2001; Keenan et al., 2014; Wu et al., 2016; Piao et al., 2019; Ma et al., 2022). With the rapid development of remote sensing technologies, there is an ever-increasing archive of satellite LSP data with global coverage, such as the Moderate Resolution Imaging Spectroradiometer (MODIS). These have greatly benefited LSP research (Piao et al., 2019), but are limited by their technical and scientific approaches and resulted in retrieval failure or low accuracy in many ecosystems including arid/semi-arid, evergreen, and urban areas (Li et al., 2017; Bolton et al., 2020; Xie et al., 2022a).

LSP is typically retrieved from vegetation index (VI) time-series measurements such as the enhanced vegetation index (EVI) and the normalized difference vegetation index (NDVI) (Baumann et al., 2017; Peng et al., 2017a) or canopy structure measurements like leaf area index (LAI) (Bornez et al., 2020). Ground-based measurements are commonly used to validate or cross-compare with satellite LSP estimates, including eddy covariance (EC) flux tower time-series measurements (Peng et al., 2017b; Zhang et al., 2018) such as OzFlux towers (Beringer et al., 2022), multispectral images from phenocams mounted on flux towers (Richardson et al., 2018) and observations provided by citizen science (Delbart et al., 2015).

The two major approaches used to determine LSP metrics from time-series data are threshold-based methods and curve-fitting methods (Cao et al., 2015). Threshold-based approaches define LSP metrics based on the date when a VI reaches a predefined absolute threshold or specific percentage (e.g., 20 %) of its annual amplitude (i.e. maximum VI minus minimum VI) (Lloyd, 1990; White et al., 1997). On the other hand, curve-fitting approaches commonly focus on changing characteristics in the time series data, with the assumption that the vegetation growth curve follows a relatively well-defined temporal pattern and can be fitted by a predefined mathematical function (e.g., sigmoid function) (Zhang et al., 2003, 2006). The effectiveness of curve-fitting algorithms depends on the assumption that vegetation growth follows a well-defined S-shaped temporal profile, which would suffer in arid and semi-arid ecosystems where irregular phenological cycles may not follow this curve (Cao et al., 2015). In contrast, threshold-based algorithms must be able to account for larger variation in phenology timing, length, amplitude, and reoccurrence interval to suit a wide variety of growing cycles (Eamus et al., 2016).

Most LSP studies to date have focused on the Northern Hemisphere, where LSP is primarily driven by seasonal changes in temperature and day length (Thompson and Paull, 2017; Zhang et al., 2018; Bolton et al., 2020; Peng et al., 2021; Zhou et al., 2022), whilst vegetation phenology in many southern ecosystems is highly associated with rainfall, e.g. arid and semi-arid areas in Australia and Africa (Brown et al., 2010; Morton et al., 2011; Xie et al., 2022a). The MODIS land cover dynamics product MCD12Q2 provides global LSP metrics, first generated using a curve-fitting approach in Collection 5 product (Zhang et al., 2003, 2006), then updated to Collection 6 product using a threshold-based method (Gray et al., 2019). But both approaches in the MCD12Q2 fail to retrieve LSP in ecosystems with a highly variable and unpredictable climate or low seasonal amplitudes.

LSP retrieval is challenging in ecosystems where the vegetation does not show strong seasonal cycles, such as in arid and semi-arid ecosystems, evergreen forests, and tropical savannas, which comprise over 30 % of global terrestrial ecosystems. The absence of vegetation phenology information in these ecosystems has significantly impeded our understanding of global ecosystem productivity and climate change impacts on terrestrial ecosystems. The Australian continent in particular possesses a range of different climate zones with aseasonal or low amplitude cycles (Hughes, 2011). Many Australian ecosystems also experience irregular and extreme events including fire, flooding, and drought, which can alter the structure, functioning, and composition of ecosystems just as much as seasonal climate (Moore et al., 2016). Therefore, Australia is an ideal study region for developing better LSP retrievals, which is the primary aim of this research. To achieve this aim, the objectives of this paper are to: (1) evaluate phenology retrieval of a new AUStralian Land Surface Phenology (AUS LSP) that improves spatial coverage of LSP information across the full range of Australian climate zones; (2) determine how phenology cycles differ among major vegetation types and over difference climatic years, including shrublands, grasslands, savannas, evergreen forests, deciduous and mixed forests; and (3) explore the potential ecological and agricultural application of the LSP metrics at a landscape scale.

2. Methods

2.1. Study area and materials

Based on a modified Köppen classification (Stern et al., 2000) and topography, land cover and land use, Australia was classified into six broad climate classes of equatorial, tropical, subtropical, arid, semi-arid, and temperate (Fig. 1). Within these climate classes, Australia supports a diverse range of land cover types including shrublands (58.0 %), grasslands (23.6 %), savannas (8.7 %), croplands (3.6 %), evergreen forests (3.4 %), deciduous and mixed forests (0.1 %). These land cover types were derived from the MCD12Q1 International Geosphere–Biosphere Programme (IGBP) land cover classification (Sulla-Menashe and Friedl, 2018) (Fig. 1 b). In general, the arid and semi-arid areas were dominated by shrublands, grasslands, and savannas, whilst equatorial, tropical, and subtropical areas were dominated by grasslands and savannas and temperate areas were covered mostly by grasslands, croplands, and forests.

We used EVI as the input data to extract LSP metrics, similar to the global product MCD12Q2 Collection 6 (Zhang et al., 2006), hereafter referred to as the global product. EVI is a normalized ratio of reflectance bands with a practical range of 0 to 1. Higher values result from absorption in the visible red band of the electromagnetic spectrum. The index correlates strongly with chlorophyll content and photosynthetic activity (Huete et al., 2002). The AUStralian Land Surface Phenology (AUS LSP) was extracted from the 16-day composite MODIS vegetation index data MYD13A1 at 500 m resolution EVI time-series for each pixel. The nineteen MYD13A1 tiles that cover the Australian landmass (h27v11, h27v12, h28v11, h28v12, h28v13, h29v10, h29v11, h29v12, h29v13, h30v10, h30v11, h30v12, h30v13, h31v10, h31v11, h31v12, h31v13, h32v10, h32v11) were downloaded from NASA (https://e4ftl01.cr.usgs.gov/). AUS LSP metrics were extracted annually from 2003 to 2018 at 500 m resolution.

2.2. LSP extraction

Before extracting the LSP metrics from the EVI time series, we

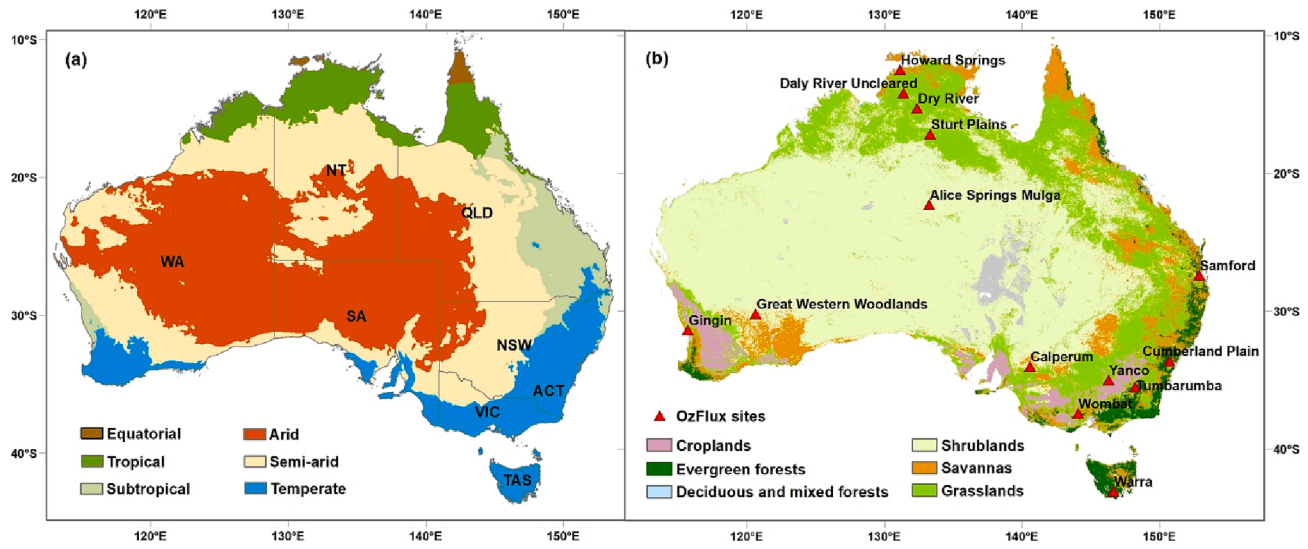

Fig. 1. (a) Australian climate classification maps. ACT: Australian Capital Territory; NT: Northern Territory; NSW: New South Wales; QLD: Queensland; TAS: Tasmania; VIC: Victoria; WA: Western Australia; (b) Land cover map of Australia and locations of 14 OzFlux sites. Legend shows major plant types according to the IGBP map in 2018. Evergreen forests are Evergreen Needleleaf Forests and Evergreen Broadleaf Forests; Deciduous and mixed forests are Deciduous Needleleaf Forests, Deciduous Broadleaf Forests, and Mixed Forests; Shrublands are Closed Shrublands and Open Shrublands; Savannas are Woody Savannas and Savannas.

performed quality control on the EVI data using the quality assurance (QA) flags provided along with the EVI data. We discarded low quality observations defined by the QA flags, which included cloudy conditions, pixels not produced, pixels indicated as not useful, and pixels with high aerosol, mixed clouds present, or adjacent cloud detected (Didan et al., 2015). We then gap-filled the low quality data using climatology values from 2002 to 2019 (Dougherty et al., 1989). Despite the 16-day composite MYD13A1 images being nominally equidistant in time (one image every 16 days), EVI values can be acquired on any day within each 16-day compositing period. To mitigate the influence of such uncertainty of temporal resolution on the extraction of phenological metrics, we adjusted the MODIS EVI time series with actual acquisition dates provided by the "Composite day of the year" band in MYD13A1 so that the EVI data was interpolated to the periodic 16-day timestamp provided. Finally, we smoothed the EVI time series using the Savitsky-Golay (SG) method to further reduce any remaining noise using a window size of 11 input data composite periods and a 3rd order polynomial (Savitzky and Golay, 1964).

We retrieved the LSP metrics in each year by including the second half of the previous year, current year, and the first half of the next year. Among current algorithms as mentioned in the introduction, threshold algorithm suits the irregular phenological patterns in Australia the best (Broich et al., 2014). For each pixel in the EVI time-series, we retrieved eight LSP metrics using a modified threshold algorithm that could further improve phenological retrieval in Australia over the global MCD12Q2 algorithm (Xie et al., 2022a). These metrics were the start, peak, end and length of each growing season, the minimum EVI value prior to and after the growing seasons, and the seasonal maximum and integral EVI values. For this study, "growing season" refers to the growing cycle of vegetation, rather than the climatological seasons such as spring and summer. The peak of growing season (PGS) was defined as the date when the EVI reached its peak value during the growing season. The start of growing season (SGS) was defined as the date when EVI reached the value that equals the minimum value prior to the PGS (min-prior) plus 20 % of the amplitude (peak EVI value minus min-prior). Similarly, the end of growing season (EGS) was defined as the date when EVI reached the value that equals the minimum value after the PGS (min-after) plus 20 % of the amplitude (peak EVI value subtracted by min-after). The length of growing season (LGS) was the period from SGS to EGS. The minimum EVI value prior to/after the growing season and the seasonal peak EVI value were also reported. Integrated EVI was calculated as the sum of all EVI values between SGS and EGS. These metrics also allowed us to calculate the seasonal amplitude (peak EVI value minus the average of min-prior and min-after). We accounted for up to two growing seasons per year and discarded those seasons with maximum EVI values that were below the average value of the entire EVI time series to avoid spurious peaks (peaks that are too low to be wide-scale growing seasons). A second season may occur for some ecosystems, which can be driven by a mixture of cool season and warm season grasses, rainfall driven growth of shrubs, forest understories, or double cropping (Broich et al., 2015; Xie et al., 2022b). Here, we primarily demonstrate and evaluate the first season as usually it is the major growing season, here the first and second season were names based on chronology. Fig. 2 summarizes our workflow for the AUS LSP retrieval, including input data, data preprocessing, LSP extraction, and output data (LSP metrics images at 500 m resolution).

2.3. Evaluation of the AUS LSP

2.3.1. Demonstration of the AUS LSP maps and cross-comparison with the global product

Using the global product as a benchmark, we compared the 2016 maps from both the global product collection 6 of MCD12Q2, referred to hereafter as the global product, and our AUS LSP maps. This year was chosen because it was one of the wettest years between 2003 and 2018 with high rainfall totals at the national scale (https://www.bom.gov.au/), and therefore yielded the best spatial coverage from the global product that as mentioned previously, often fails to detect dryland vegetation that may lie dormant in dry years (Ma et al., 2013). The success rate of retrieval of phenological metrics, defined as the percentage of pixels with phenological information, was calculated to evaluate the performance of AUS LSP. We calculated the success rate of retrieval for both AUS LSP and the global product for each of the vegetation type (Fig. 1 b), based on the proportion of pixels that yielded LSP retrievals among all pixels within the same vegetation type.

2.3.2. Demonstration of the AUS LSP at selected sites and cross-comparison with seasons derived from eddy covariance data

To evaluate our algorithm, we used 14 sites within the OzFlux network (Beringer et al., 2022) which provide continuous observation of ecosystem carbon, water and energy fluxes and climate using the eddy covariance (EC) method. The 14 sites chosen represented major

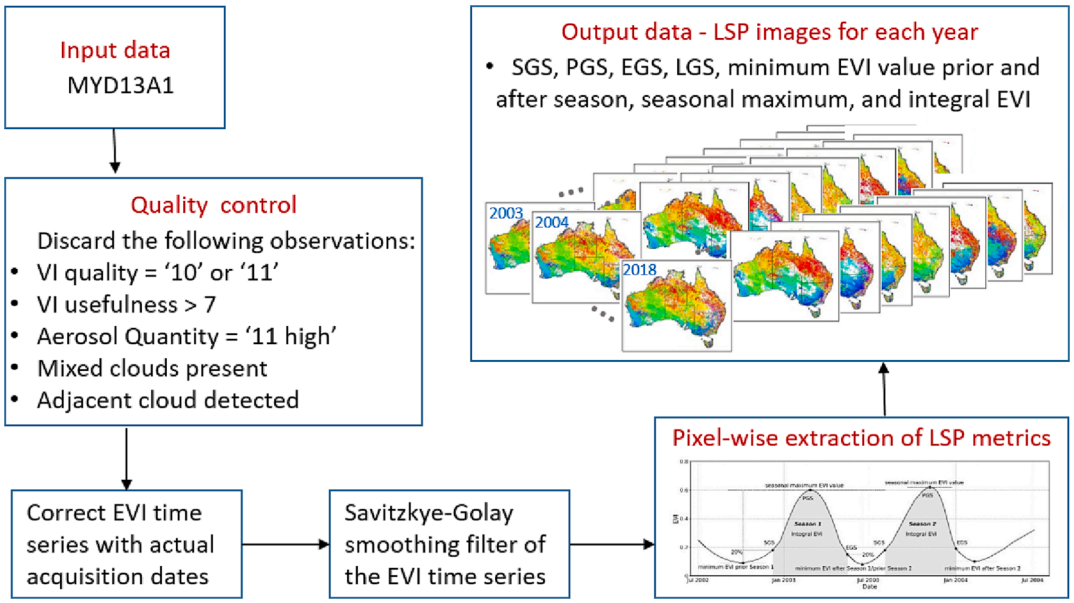

Fig. 2. Workflow of the AUStralian Land Surface Phenology (AUS LSP) retrieval process.

vegetation types across different climate zones in Australia, including six sites in arid and semi-arid areas and eight sites in tropical, subtropical, and temperate areas (Table 1, Fig. 1 b).

EC flux towers yield valuable *in situ* observations on the seasonal dynamics and inter-annual variations of net ecosystem exchange (NEE) between the land surface and the atmosphere (Baldocchi et al., 2001), which can be partitioned into its major fluxes of gross primary productivity (GPP, i.e., the sum of the net photosynthesis by all leaves measured at the ecosystem scale) and ecosystem respiration (ER) (Isaac et al., 2017) and used to evaluate satellite vegetation functional products including land surface phenology (Chapin et al., 2006). Individual site setup, including detailed vegetation descriptions and instrumentation can be found via the corresponding site reference provided in Table 1. The EC data were obtained from the OzFlux data portal (Beringer et al., 2022), which supplies data that are quality checked and quality assured (level 3 standard) by the respective site leader. Once obtained for this study, these data were processed to obtain a complete time-series of GPP using the PyFluxPro tool that was developed by the OzFlux community as describe in detail by Isaac et al (2017). In brief, the meteorological data provided with each site file were gap filled using

Table 1
Names, locations, land cover, climate zone, annual mean temperature (AMT) and annual precipitation (AP) averaged from 2003 to 2018, and gross primary productivity (GPP) data coverage of the OzFlux sites shown in Fig. 1.

Site name	Lat(°S)	Lon(°E)	Site description	Land cover	% of land cover	Climate	AMT (°C)	AP (mm)	GPP data	Reference
Great Western Woodlands [AU-GWW]	30.191	120.654	Temperate Eucalypt woodland	Savannas	8.7 %	arid	20	343	2013–2019	(MacFarlane, 2013)
Alice Springs Mulga [AU-ASM]	22.275	133.225	Acacia woodland & hummock grassland	Shrublands	58.0 %	semi-arid	23	390	2011–2019	(Cleverly, 2011)
Calperum [AU-Cpr]	34.003	140.588	Mallee woodland	Shrublands	58.0 %	semi-arid	18	270	2011–2019	(Tech, 2013)
Yanco [AU-Ync]	34.989	146.291	Grassland	Grasslands	23.6 %	semi-arid	17	418	2013–2019	(Beringer, 2013a)
Sturt Plains [AU-Stp]	17.151	133.350	Mitchell grassland	Grasslands	23.6 %	semi-arid	27	730	2009–2019	(Beringer, 2013b)
Dry River [AU-Dry]	15.259	132.371	Open forest savanna	Grasslands	23.6 %	semi-arid	27	991	2009–2019	(Beringer, 2013c)
Howard Springs [AU-How]	12.494	131.152	Tropical savanna	Savannas	8.7 %	tropical	28	1715	2002–2019	(Beringer, 2013d)
Daly River Uncleared [AU-DaS]	14.159	131.388	Woodland savanna	Grasslands	23.6 %	tropical	28	1233	2008–2019	(Beringer, 2013e)
Gingin [AU-Gin]	31.376	115.714	Banksia woodland	Savannas	8.7 %	subtropical	19	609	2012–2019	(Silberstein, 2015)
Samford [AU-Sam]	27.388	152.884	Pasture	Savannas	8.7 %	subtropical	20	1158	2011–2017	(Rowlings, 2011)
Cumberland Plain [AU-Cum]	33.615	150.724	Dry sclerophyll forest	Evergreen Broadleaf Forest	2.9 %	temperate	18	758	2013–2019	(Pendall, 2015)
Tumbarumb-a [AU-Tum]	35.657	148.152	Wet sclerophyll forest	Evergreen Broadleaf Forests	2.9 %	temperate	14	901	2002–2019	(Woodgate, 2013)
Warra [AU-Wrr]	43.085	146.656	*Eucalyptus obliqua* forest	Evergreen Broadleaf Forests	2.9 %	temperate	8	1641	2013–2019	(Phillips, 2015)
Wombat [AU-Wom]	37.422	144.094	*Eucalyptus obliqua* forest	Evergreen Broadleaf Forests	2.9 %	temperate	12	783	2010–2019	(Arndt, 2013)

the SOLO (self-organising linear output) neural network model (Hsu et al., 2002), available in PyFluxPro, which was trained with gridded surface layer ERA5 data (ECMWF Reanalysis 5th Generation) from the European Centre for Medium Range Weather Forecasting (ECMWF) (Hersbach et al., 2017) and weather data from nearby Australian Bureau of Meteorology stations. For NEE, water and energy, the data were filtered using a site and year specific friction velocity threshold (u*), which is standard practice used to remove fluxes during low turbulence (Barr et al., 2013). The data were then gap filled using the SOLO model with meteorological variables as inputs to create complete time-series of carbon (i.e. NEE), water and energy fluxes (Isaac et al., 2017). Lastly, to partition NEE into GPP and ecosystem respiration (ER), night-time NEE fluxes (ER only) were used to apply a nocturnal temperature response function (Lloyd and Taylor, 1994) using the SOLO model to determine ER. GPP was then calculated as NEE subtracted by ER. To keep the temporal resolution consistent between the EVI and GPP data, daily GPP was averaged using a 16-day window that corresponded to the 16-day resolution MODIS EVI observations. For each OzFlux site, we used the same algorithm as used for EVI data to extract phenological timing metrics (SGS, PGS, and EGS) from the GPP time series. We then compared these LSP timing metrics generated using satellite EVI data and EC GPP data, which is a common practice to evaluate satellite-derived LSP (Peng et al., 2017a; Kato et al., 2021; Zhao et al., 2022). This approach allowed us to confirm whether growing seasons generated from EVI data were real/widescale seasons rather than spurious seasons, as well as the percentage of growing season number confirmed by those shown from GPP was calculated as an indicator of accuracy.

2.3.3. Phenology of major vegetation types in Australia using the AUS LSP

We explored the phenological patterns of the major vegetation types in Australia using our AUS LSP generated from MODIS EVI data. SGS, PGS and EGS histograms in each year were calculated for each vegetation type, i.e., shrublands, grasslands, savannas, croplands, evergreen forests, and deciduous and mixed forests, respectively. Then the histograms were averaged across 16 years from 2003 to 2018 to show the climatology of growing seasons.

To show the contrast of phenology in extremely wet and dry years, we calculated the histogram of integral EVI, an approximation of productivity, for shrublands and grasslands in a wet year (2011) and in a dry year (2018) according to annual rainfall provided by the Australian Bureau of Meteorology. Total productivity of shrublands and grasslands across Australia was calculated by adding up the integral EVI value of all shrubland and grassland pixels, respectively.

3. Results

3.1. Demonstration of AUS LSP and cross-comparison with the global product

Fig. 3 demonstrates the three phenological timing metrics start, peak, and end of growing season (SGS, PGS, EGS), shown for the first season in 2016 (one of the wettest years) generated from the global product (Fig. 3 a–c) and the AUS LSP (Fig. 3 d-f). For both the global and the AUS LSP retrievals, growing seasons generally started and ended earlier in the north where the climate is warmer, compared to the south where the climate is cooler. Through visual comparison, the global product (Fig. 3 a-c) showed a high consistency with the AUS LSP (Fig. 3 d-f) in areas where both the global product and our algorithm retrieved LSP values, whilst the AUS LSP provided more retrievals in arid/semi-arid areas covered by shrublands, grasslands and temperate areas covered by evergreen forests (cf. Fig. 1) where the global product showed missing values.

For each of the six major vegetation types (Fig. 1 b), shrublands showed the lowest seasonal amplitude according to AUS LSP metrics (Fig. 4 a), followed by evergreen forests, savannas, grasslands, deciduous forests and croplands. These generally agree with the patterns of success rate of retrieval for the global product and AUS LSP as shown in Fig. 4 b, i.e., both the global product and AUS LSP showed the lowest success rate of retrieval in shrublands, and the highest in croplands. This pattern was confirmed by the significant correlation between the average amplitude of each vegetation type and the success rate (Fig. 4 c), with the success rate of the global product significantly associated with the amplitude ($r = 0.88$, $p = 0.02$), and a similar, though not significant, association for AUS LSP ($r = 0.80$, $p = 0.06$). On the other hand, the AUS LSP showed higher overall success rate of retrieval (Fig. 4 a, b), particularly for vegetation with low seasonal amplitudes (EVI < 0.1), including shrublands (9 % success rate for the global product and 74 % for AUS LSP), evergreen forests (21 % success rate for the global product and 75 % for AUS LSP), and savannas (32 % success rate for the global product and 86 % for AUS LSP). And across 16 years from 2003 to 2018, AUS LSP provided information that covers 70 % of Australia on average, which was a significant improvement compared to the 26 % success rate

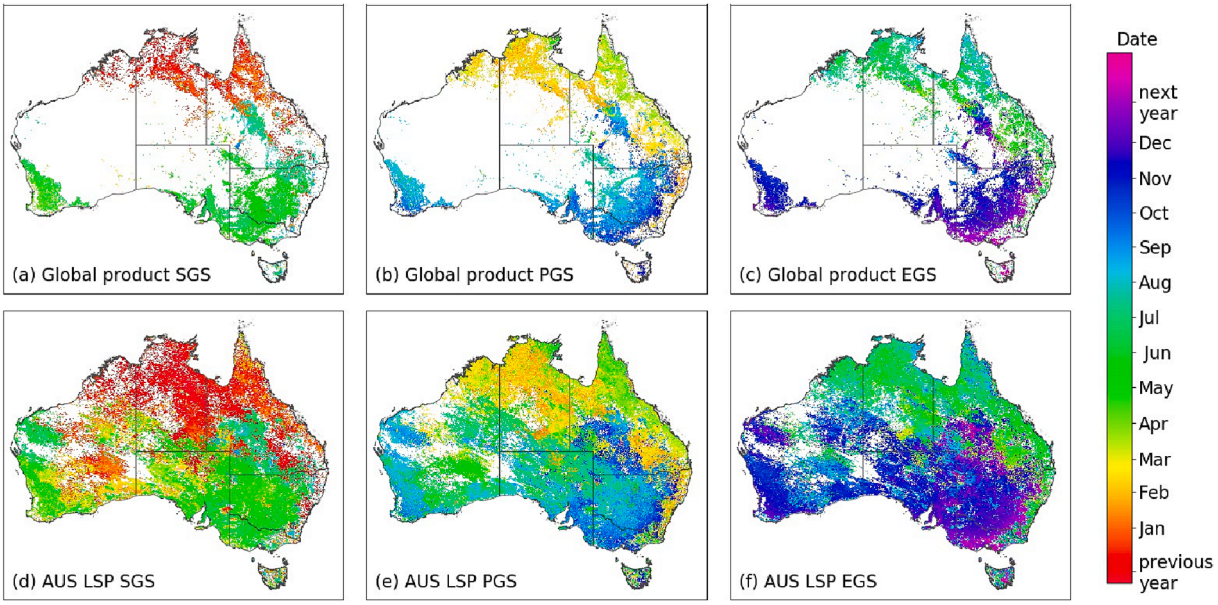

Fig. 3. SGS, PGS, and EGS of the first season in 2016 from the global product and the AUS LSP. White pixels represent areas without detectable vegetation growth.

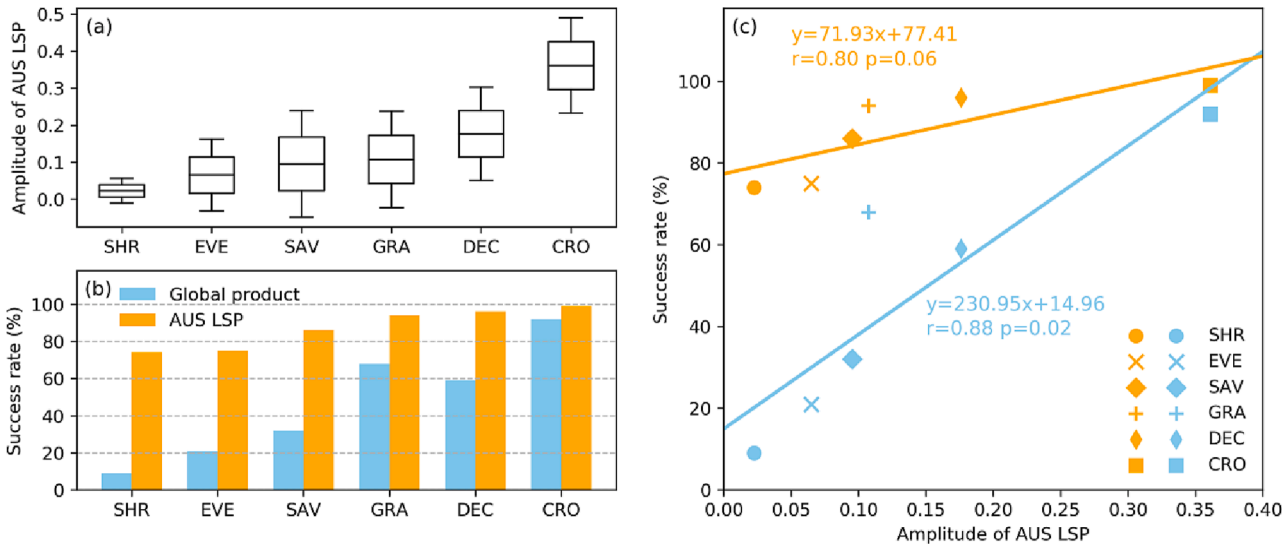

Fig. 4. Amplitude (generated from AUS LSP) and success rate of the global product and AUS LSP in each vegetation type for the first season in 2016: SHR (shrublands), EVE (evergreen forests), SAV (savannas), GRA (grasslands), DEC (deciduous and mixed forests), CRO (croplands). (a) Seasonal amplitude for each vegetation type: average and standard error of all pixels within the same vegetation type; (b) Success rate of retrieval in each vegetation type from the global product and the AUS LSP; (c) Correlation between the success rate of retrieval and amplitude (average value of all pixels within the same vegetation type) generated from AUS LSP.

of the global product.

Further quantitative comparison in Fig. 5 confirmed the reliability of AUS LSP as it showed a high degree of consistency with the global product for pixels where both retrievals are available. In both mesic (equatorial, tropical, subtropical, and temperate areas as shown in Fig. 1 a) and arid/semi-arid areas, most SGS/PGE/EGS retrievals showed a difference within 16 days between AUS LSP and the global product observations. The PGS retrievals from both datasets agree very well with each other with the differences centred at 0 (Fig. 5 b). We noted that the SGS retrievals from AUS LSP were slightly earlier than those from the global product with the differences centred between 0 and −16 days (Fig. 5 a), and the PGS retrievals from AUS LSP were slightly later than those from the global product with the differences centred between 0 and 16 days (Fig. 5 c).

3.2. *Illustration of the input and output data of the LSP retrieval algorithm and validation of the LSP metrics at selected sites*

We illustrated the input EVI time series (MODIS original EVI time series and EVI time series after quality control, regularization of acquisition dates, and SG filtering) and key output LSP metrics (SGS, PGS and EGS) of the retrieval algorithm at the OzFlux EC sites (Fig. 6), as well as the *in situ* measurement of vegetation dynamics GPP and LSP metrics retrieved using GPP data.

Both EVI and GPP time series at the OzFlux sites showed very distinct seasonality between different vegetation types across different climate zones. The two semi-arid shrubland sites (Calperum, Alice Springs Mulga) and an arid savanna site (Great Western Woodlands) (Fig. 6) show that phenology of shrublands and savannas in arid/semi-arid areas could be highly irregular in terms of phenological timing and EVI amplitude; for example, at the Alice Springs Mulga site, no growing season was extracted in 2013 whilst two growing seasons were detected in 2017 and the seasonal amplitude in 2017 was much higher than in other years. The other three savanna sites showed increasing seasonal amplitude as the annual rainfall increases from the sub-tropical sites (Gingin, Samford) to the tropical site (Howard Springs). The four evergreen forest sites are all in temperate zones, among which two evergreen sclerophyll forest sites (Cumberland, Tumbarumba) show high EVI values throughout the year with low seasonal amplitude, and the other two evergreen eucalypt forest sites (Wombat, Warra) show higher seasonal amplitude with PGS in summer (December – February). The four semi-arid grassland sites show diverse phenology, with seasonal peaks at Sturt Plains in late summer (February) and those at Yanco in late winter to early spring (August – September).

As shown in Table 2, for the six sites in arid/semi-arid areas, on average, 96 % of growing seasons generated from satellite EVI matched

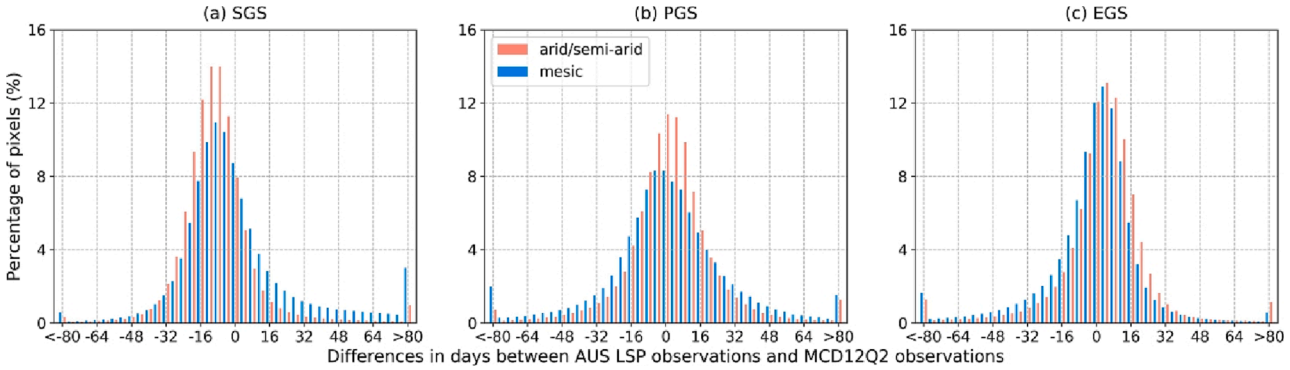

Fig. 5. Differences in days between SGS/PGS/EGS observations from AUS LSP and the global product MCD12Q2 in mesic areas (blue bars) and arid/semi-arid areas (red bars) for the first season in 2016. (For interpretation of the references to colour in this figure legend, the reader is referred to the web version of this article.)

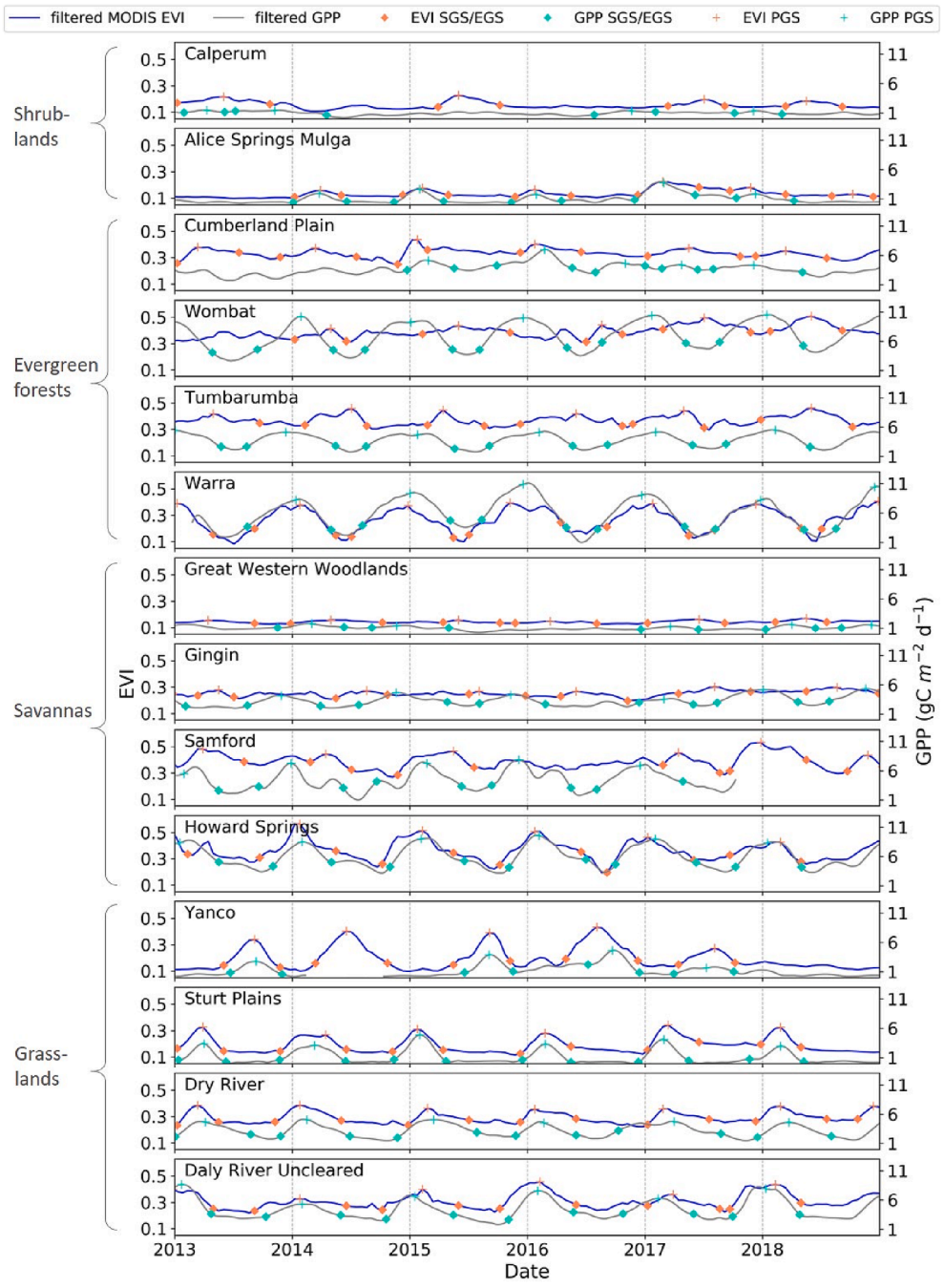

Fig. 6. EVI/GPP time series (input data of the LSP retrieval model) and characterized LSP episodes (output data of the LSP retrieval model) across from 2013 to 2018 at 14 OzFlux sites that represent different vegetation types across different climate zones. Sites within the same vegetation type were sorted according to annual rainfall amount with the top one having the lowest annual rainfall.

with those generated from EC GPP, i.e. GPP observations confirmed that those growing seasons observed by satellite EVI were real/widescale growing seasons; for the eight sites in tropical, subtropical, and temperate areas, 90 % of growing seasons generated from satellite EVI matched with those generated from EC GPP. Per vegetation type, on average, 94 %, 85 %, 95 %, 98 % of the satellite EVI growing seasons matched with those generated from EC GPP in shrubland, evergreen forest, savanna, and grassland sites, respectively.

3.3. LSP of major vegetation types

Fig. 7 presents the frequency/number of pixels (averaged across 16 years from 2003 to 2018) of the SGS, PGS and EGS of for the growing seasons of evergreen forests, deciduous and mixed forests, shrublands, savannas, grasslands, and croplands (cf. Fig. 1). For most shrublands, grasslands and savannas, the growing seasons started during summer (December – February), reached PGS during autumn (March to May), and ended during winter (June – August). In addition, grasslands consisted of warm season (generally C_4) and cool season (generally C_3) grasses, and we detected two obvious periods of growing seasons peaking in autumn (March – May) and spring (September – November), respectively. The histograms also revealed that croplands in Australia are dominated by winter crops, with most of cropland pixels reaching their peak of growing season in late winter to early spring (August – October). Evergreen forests show active growing seasons all year round. In contrast, deciduous forests mostly reached the PGS in spring

Table 2
Number of growing seasons (GS) extracted using EVI and GPP, respectively.

Site name	GS generated using AUS LSP compared with those generated using EC GPP		
	Years when both data were available	No. of GS from AUS LSP	% of GS confirmed by those from GPP
Great Western Woodlands [AU-GWW]	5	5	100 %
Alice Springs Mulga [AU-ASM]	8	8	88 %
Calperum [AU-Cpr]	8	6	100 %
Yanco [AU-Ync]	5	4	100 %
Sturt Plains [AU-Stp]	9	9	100 %
Dry River [AU-Dry]	10	10	90 %
Howard Springs [AU-How]	16	16	94 %
Daly River Uncleared [AU-DaS]	9	9	100 %
Gingin [AU-Gin]	7	7	86 %
Samford [AU-Sam]	8	9	100 %
Cumberland Plain [AU-Cum]	5	5	80 %
Tumbarumba [AU-Tum]	15	15	87 %
Warra [AU-Wrr]	5	6	83 %
Wombat [AU-Wom]	9	8	88 %
Average of shrubland sites	–	–	94 %
Average of evergreen forest sites	–	–	85 %
Average of savanna sites	–	–	95 %
Average of grassland sites	–	–	98 %
Average of arid /semi-arid sites	–	–	96 %
Average of mesic sites	–	–	90 %

(September – November).

The LSP metrics allowed us to explore the variation in phenology between years with opposite climate extremes. Fig. 8 contrasts integral EVI, an approximation of productivity, in a wet year for (2011) and a dry year (2018) for Australian shrublands and grasslands. These are the two vegetation types with the widest coverage among the six vegetation types mentioned above and dominate the arid and semi-arid areas, which are influenced by rainfall more than other mesic ecosystems. In the wet year, not only did more shrubland and grassland pixels show active growing seasons compared to the dry year, but also the productivity of these systems was much higher. Note that the total productivity of shrublands in the wet year (27.5 million integral EVI) was nearly-four times the amount of that in the dry year (7.7 million integral EVI).

4. Discussion

4.1. Evaluation of the algorithm

4.1.1. Algorithm performance

The implementation of our algorithm across Australia demonstrated its enhanced ability to detect LSP metrics across various ecosystems that exist on the continent. Compared to the global product, our algorithm improved spatial coverage of the LSP retrieval in arid/semi-arid shrublands and grasslands, semi-arid savannas, tropical and sub-tropical areas, and temperate evergreen forests. AUS LSP provided retrievals across these systems where the current global product retrieved no data, whilst maintaining the accuracy of retrievals as shown by high consistency with the global product where both provided retrieval values (Fig. 3, Fig. 5). At 14 EC flux tower sites, around 96 % of the number of growing seasons in arid/semi-arid areas and 90 % of the number of growing seasons in mesic areas from AUS LSP were confirmed by those derived from EC tower GPP measurements (Table 2).

The difference in algorithm threshold could be a major cause of such difference between AUS LSP and the global product. The global product used a threshold algorithm that required the seasonal amplitude to be at least 0.1, whilst our algorithm used a threshold algorithm that instead required the peak EVI value to be above or equal to the average of time series EVI across 16 years. The global product missed LSP information in most low seasonal amplitude ecosystems including shrublands, evergreen forests, and savannas (Fig. 4), providing LSP retrievals in<26 % of continental Australia. Our algorithm improved the detection of LSP and provided LSP retrievals in 70 % of the continent. For example, as shown in Fig. 6, shrublands (as seen at Calperum and Alice Springs Mulga), temperate evergreen forests (as seen at Cumberland Plain and Tumbarumba), and savannas (as seen at Gingin and Great Western Woodlands) can have very low seasonal amplitudes; as such, these growing seasons could be missed by the global product when the amplitude is lower than 0.1. Shrublands and savannas in arid/semi-arid ecosystems also showed more irregular phenology with low seasonal dynamics and growing seasons that could skip a year or occur more than once a year. For example, as shown in Fig. 6, Alice Spring Mulga did not show any growing season in 2013 but showed two growing seasons in 2017 according to flux tower GPP derived phenology. Likewise, Great Western Woodlands showed two growing seasons in 2014 but did not show any growing seasons in 2015 and 2016. Tropical/sub-tropical savannas and temperate evergreen forests showed generally higher greenness (EVI) values but low seasonal amplitude, as show at Cumberland Plain, Tumbarumba, and Gingin (Fig. 6). These examples of low seasonal amplitude systems pose great challenges in LSP retrieval. Thus our algorithm improved LSP retrieval and provided phenological metrics for these critical ecosystems. Such information, missed by the global product, is key to understanding global water and carbon cycles (Cleverly et al., 2016b; Wang et al., 2019). For example, temperate areas, particularly evergreen forests, have the highest mean net primary production across Australia despite their relatively low proportional area of the continent at ~ 3 %, (Haverd et al., 2013). Likewise, vegetation in arid/semi-arid Australia has been estimated to contribute around half of the anomalous increase in global land carbon sink observed in wet years such as 2011 (Poulter et al., 2014; Cleverly et al., 2016a).

Previous studies found that phenology detectability is associated with vegetation cover within shrubland ecosystems, i.e., higher vegetation cover is easier for phenology detection (Peng et al., 2021), suggesting that phenology retrieval is challenging in areas with low vegetation greenness, such as in arid and semi-areas. Retrieving LSP in evergreen ecosystems using optical remote sensing methods is also challenging, both technically and scientifically (Bolton et al., 2020), because the low dynamic range of these ecosystems make it difficult to detect the phenological cycles and the interpretation of retrieved phenological metrics may be ambiguous. By investigating LSP across diverse ecosystems including shrublands, savannas, grasslands, forests, and croplands, our study revealed that the detectability of LSP increases as the growing season amplitude increases (Fig. 4), regardless of their vegetation cover (evergreen forests have high vegetation cover/greenness, whilst shrublands have low vegetation cover/greenness). In other words, when focused on multiple ecosystems, the phenology detectability is not necessarily associated with vegetation cover, contrast to the findings of Peng et al (2021). Rather, our findings agree with Bolton et al (2020) that LSP retrieval algorithms require technical improvement in evergreen ecosystems in order to retrieve LSP information. Although we successfully retrieved LSP in temperate evergreen forests and the metrics were validated by flux tower measurements at 4 sites, the phenological information needs further validation and careful interpretation. The phenological changes could be driven by grasslands under the tree canopy, or deciduous trees amongst the evergreen trees within one pixel. Note that phenology detectability is also associated with satellite image resolution. Thus for urban vegetation phenology

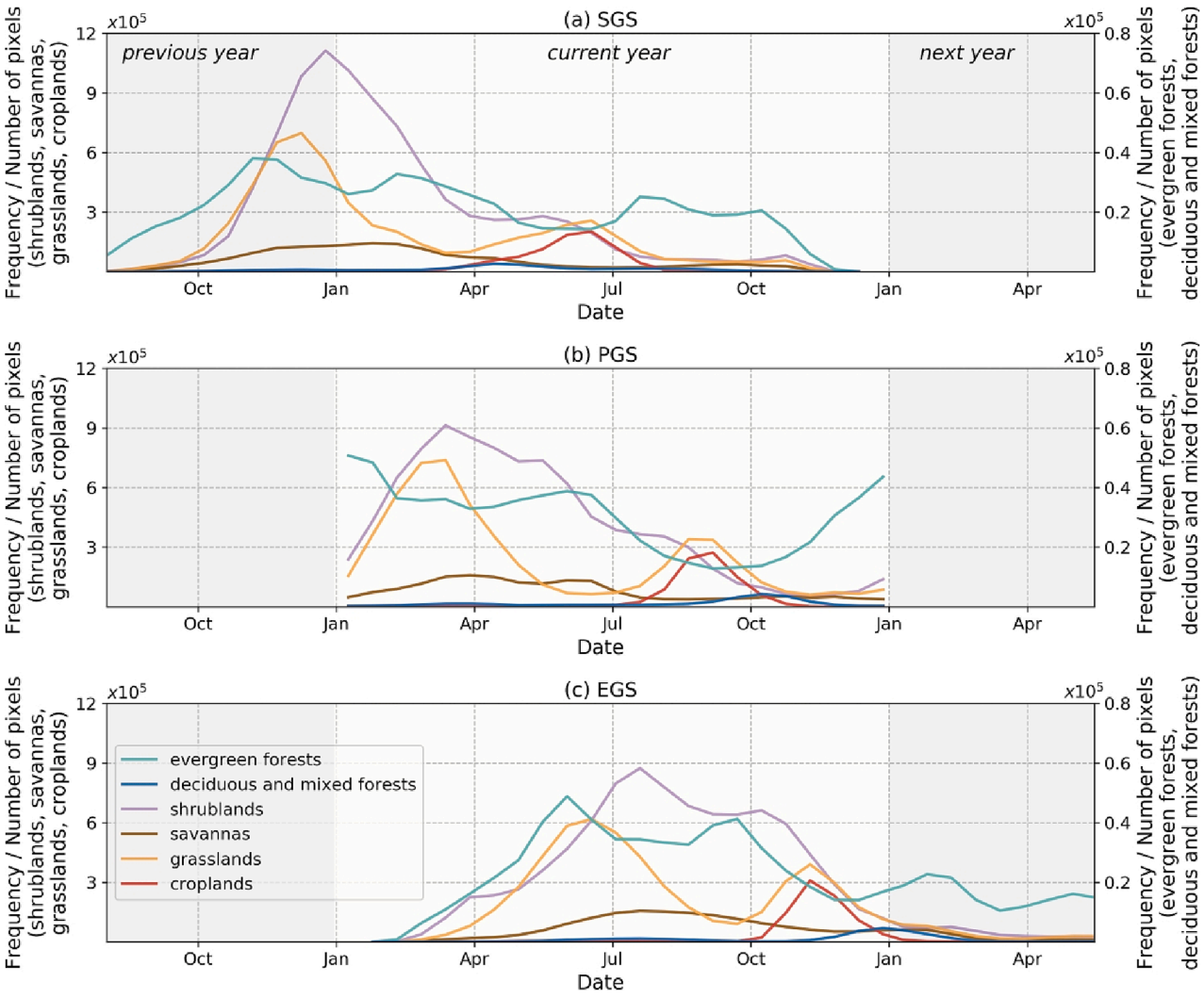

Fig. 7. Start (SGS), peak (PGS), and end (SGS) of growing seasons for six major vegetation types, based on average histogram from 2003 to 2018.

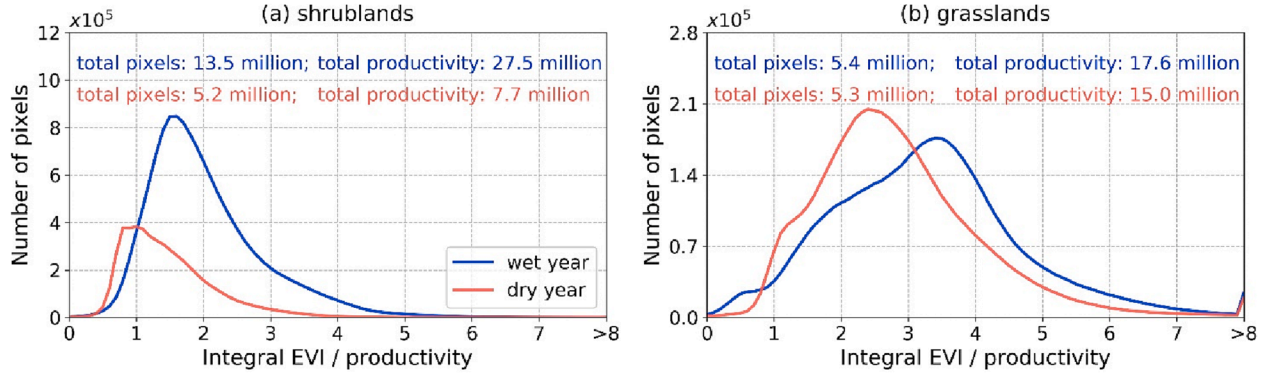

Fig. 8. Histogram of integral EVI (productivity) of the first growing season in a wet year (2011) and a dry year (2018) for shrublands, and grasslands. Total productivity was calculated by adding the integral EVI of all pixels, as introduced in Methods.

retrieval, the main challenge is that the urban vegetation is smaller in spatial scale and more complex in spatial pattern, which cannot be fully captured by the 500 m MODIS data used in our study (Li et al., 2017).

4.1.2. *Limitations of the algorithm*

Notwithstanding its advantages, we acknowledge that the AUS LSP poses several practical challenges. We organised the LSP metrics by calendar year, in spite of the fact that there is no ideal twelve-month interval for organizing phenology data in Southern Hemisphere, where many plants start their season just before the beginning of a calendar year (Broich et al., 2015). Fig. 7 demonstrates that growing seasons of vegetation across Australia can occur at any time of year (e.g. evergreen forests), start before the beginning of a year (e.g. shrublands, grasslands, and savannas), extend across the end of a year (e.g. evergreen forests,

deciduous and mixed forests), occur more than once in a year (e.g. grasslands), or skip a year (cf. Fig. 6). Therefore, in a similar way that SGS/PGS/EGS is provided by the global product, we recommend that the derived LSP metrics in our study are best analysed in a temporally continuous manner including the previous year and the next year, i.e., to convert the day of year to number of days since the 1st of the commencing year (2003). Note that in Fig. 7, we combined all Evergreen Broadleaf Forests into one category, whilst specific application of the LSP metrics need to be associated with more detailed land cover information. For example, dry sclerophyll forest (e.g., Cumberland Plain site) is more fire-prone, compared to wet sclerophyll forest (e.g., Tumbarumba site), as the open structure of dry sclerophyll forest contributes to the drying out of fire fuels, and this facilitates the ignition of fires especially during hot and dry weather (Zhang et al., 2017).

Our algorithm avoids spurious growing seasons by using a threshold for seasonal amplitude greater than or equal to time series average EVI across 16 years. As such, LSP metrics are not produced when the threshold was not met. A limitation of this algorithm is that it could result in missing values when the amplitude of a real growing season is significantly lower than those in other years. To address this, it is important to scrutinise the data with respect to the climatic data driving the amplitude and within the ecological context of the vegetation type. It may be necessary to adjust the threshold accordingly. Additionally, the temporal resolution of our AUS LSP is limited by the temporal resolution of the input data, i.e., the 16-day MODIS EVI time series data.

In this study, we cross-compared our AUS LSP with the global product for evaluation of the accuracy. PGS observations from both datasets aligned well with each other, whilst average onset of growing season from AUS LSP was earlier than the global product observations, with most pixels showing a difference of around 16 days. The average EGS from AUS LSP was later than the global product observations, again with a difference of roughly 16 days. These discrepancies could be caused by the difference in temporal resolution of input data as the global product used daily EVI2 data and the AUS LSP used 16-day EVI time series data. We also compared the growing seasons generated using satellite data with those generated using OzFlux EC GPP at 14 sites and confirmed that most of the AUS LSP growing seasons were real growing seasons rather than spurious ones. We did not directly compare the LSP metrics generated using satellite data with those generated using GPP, because studies have reported that vegetation greenness does not necessarily represent primary production (Restrepo-Coupe et al., 2016). Also, there is typically a time lag between phenological observations from EVI and GPP data because EVI is a structural and greenness proxy whilst GPP is a physiological proxy of vegetation (Walther et al., 2016). For example, at the evergreen *in situ* eddy covariance sites in our study, Tumbarumba and Wombat (Fig. 6), EVI time series peaked in winter (June – August) whilst GPP time series peak in summer when the temperature increased, i.e. not necessarily caused by increasing greenness. It therefore is important to account for potential artefacts present in remotely sensed data by cross-validation with *in situ* flux data where possible (Restrepo-Couple et al., 2016). In addition, our results were optimised for Australia and compared against the global phenology product. It remains to be seen the extent to which the optimisation performed here is applicable to other areas, including at global scale.

4.2. Applications of AUS LSP

Our AUS LSP metrics characterize the timing of phenological cycles, as well as the magnitude in phenological variation in vegetation greenness (i.e., EVI), including the start (SGS), peak (PGS), end (EGS), and length (LGS) of growing seasons, minimum EVI value prior to and after the growing seasons, and seasonal maximum and integral EVI values. The quantified spatial–temporal information of vegetation growth advances our knowledge of Southern Hemisphere ecosystems, whilst most phenology studies have been focused on the Northern Hemisphere and often on boreal and deciduous forests.

The AUS LSP provides phenological information in ecosystems where such information was not available before, especially in shrublands, evergreen forests, and arid savannas ecosystems, which cover greater than 30 % of the land globally (Loveland et al., 2000). As such, this study will significantly enhance our understanding of ecosystem dynamics, carbon exchanges, future climate impacts, and fire behaviour across diverse ecosystems. These above mentioned Southern Hemisphere ecosystems deviate from the predictable seasonality of temperate and tropical deciduous biomes, and they are primarily within the arid/semi-arid areas in the interior and in the sub-humid areas in southwest and southeast Australia where rainfall variability is strong (Moore et al., 2016). With its high retrieval rate across different climate zones, AUS LSP also has the capacity to help monitor vegetation under climate variability, along the gradients of temperature and rainfall from coastal to interior land areas. For example, we were able to calculate the climatology of growing seasons and quantify the year-to-year changes in the timing and magnitude of growing seasons. The LSP metrics provide rich information that also help track ecosystem compositions. For example, the differences in phenology between Sturt Plains and Yanco grassland sites (Fig. 6) reflect the contrasting grass functional types across Australia; the grasses at Sturt Plains are dominated by warm season grasses and the grasses at Yanco are dominated by cool season grasses.

Applications of the phenological timing metrics provided by our algorithm (i.e., SGS, EGS, PGS, and LGS) include determination of the sensitivity of phenology to climate change, tracking shifts in phenology, and response of vegetation to extreme climate events. The LSP timing metrics can be analysed in a temporally continuous fashion to determine long-term trends of vegetation phenological dynamics, and to quantify the change in phenology with respect to the climatology (Tong et al., 2019; Zhang et al., 2019). These LSP metrics also allow value added information extraction, such as in-depth analysis of LSP shifts associated with land use change as well as the climate controls of those shifts (Peñuelas and Filella, 2009; Shen et al., 2015; Piao et al., 2019; Wu et al., 2021). Recently, Australia has experienced an increase in both the frequency and severity of climate extremes (King et al., 2020), e.g. heatwaves, droughts, and floods (Bureau of Meteorology and CSIRO, 2020). These threats pose severe concerns for the ecosystems ability to absorb carbon, maintain biodiversity, and support human livelihoods (Ma et al., 2016; Pörtner et al., 2022). AUS LSP can help inform studies on vegetation responses to extreme climate events, such as ecosystem resilience and recovery from disturbance.

In addition to the timing of phenological cycles, the magnitude of the metrics (i.e., minimum, maximum, and seasonal integral EVI) can be used to quantify vegetation cover and biomass, which are key to ecosystem carbon sequestration, crop yield estimation, bushfire fuel load estimation, etc. For example, the integral EVI can inform us about the photosynthetic production of each component of the ecosystem. Throughout the grasslands and shrublands that provide important ecological services such as erosion control and climate regulation (Miller et al., 2011), the improved quantification of productivity will contribute to the study of carbon and water exchange. For example, our results show that the productivity of shrublands in a wet year could be nearly-four times the productivity in a dry year (Fig. 8), which reflects a large inter-annual variation of carbon sinks in these shrublands (Cleverly et al., 2016a). In addition, the seasonal timing and biomass of these grasslands can assist in quantifying bush fire fuel load (Nolan et al., 2022), thus providing significant information for bush fire management. EVI integrated over a season can be used as a proxy of vegetation primary production and an indicator of crop yield (Xin et al., 2015; Ji et al., 2022). Our findings (Fig. 7 c) detected that croplands in Australia are dominated by winter crops with peak growing seasons from late winter (August) to early spring (September), aligning with the crop planting recommendations for Australia (ABARES, 2022). Besides the overall seasonal timing and productivity of all crops, our maps of LSP metrics enable spatially detailed tracking of how the PGS of crops is changing

from year to year, thus improving our understanding of how crop phenology across Australia's major cropping regions responds to rainfall and other climate variables.

5. Conclusion

This study presents AUStralian Land Surface Phenology (AUS LSP) annual retrieval at 500 m resolution across diverse ecosystems including arid/semi-arid, equatorial, tropical, sub-tropical and temperate zones. Using a modified threshold algorithm, we improved the spatial coverage of LSP information in Australia from only 26 % of the continent with the global product to 70 % with AUS LSP averaged across 16 years from 2003 to 2018. Evaluation using *in situ* eddy covariance gross primary productivity measurements and cross comparison with the global LSP product demonstrated the reliability of this algorithm to detect LSP metrics across different biomes in different climate zones. The ecosystems missed by the current global LSP product are mostly shrublands, savannas, and evergreen forests, because they have low seasonal amplitudes regardless of vegetation cover (shrublands and savannas in arid/semi-arid areas showed low vegetation cover/greenness, whilst tropical/sub-tropical savannas and temperate evergreen forest areas showed high vegetation cover/greenness). Our method could contribute to the LSP retrieval in these shrubland, savanna, and evergreen forest ecosystems that cover more than 30 % of the land globally. We highlight the role of seasonal amplitude in influencing LSP retrieval, whilst most current studies focused on the relationship between vegetation cover and LSP detectability, i.e., the detectability of LSP increases as the seasonal amplitude increases. Our results also revealed pronounced contrast between the productivity of the shrublands and grasslands in a wet year and in a dry year, suggesting drastic changes in carbon and water cycles in these ecosystems. This research meets the urgent need to understand how diverse ecosystems adapt to environmental variability in temperature and water availability through characterized phenological dynamics. Whilst AUS LSP successfully retrieved LSP from temperate evergreen forests, future validation work is planned in these ecosystems where LSP monitoring and interpretation remains a challenge. The rich information provided by LSP metrics and extracted information for these metrics could be applied by landscape and agricultural managers and the scientific community for analyses such as bushfire fuel accumulation, crop yield prediction, and quantifying ecosystem resilience to climate change. The algorithm used in this study for deriving LSP metrics from time series satellite greenness measurements provides a reference for other regions with diverse ecosystems, particularly those ecosystems with low variation in greenness amplitude like evergreen forests and arid shrublands and grasses and/or regions with variable and unpredictable rainfall.

Declaration of Competing Interest

The authors declare that they have no known competing financial interests or personal relationships that could have appeared to influence the work reported in this paper.

Data availability

Data will be made available on request.

Acknowledgements

This study was supported by the Australian Research Council's Discovery Projects funding schemes (DP170101630, DP210100347) and Australian landscape phenology and vegetation dynamics for climate resilience, ecosystem services, and forecasting project (CSIRO – C013420). OzFlux data were provided by TERN and supported by the Australian government through the National Collaborative Research Infrastructure Strategy (NCRIS). Qiaoyun Xie was supported by University of Technology Sydney Chancellor's Postdoctoral Research Fellowship (CPDRF). Yanling Ding was supported by the Fundamental Research Funds for the Central Universities (Project No.2412020FZ004). Xuanlong Ma was supported by the National Natural Science Foundation of China (42171305), Natural Science Foundation of Gansu Province, China (21JR7RA499) and the Director Fund of the International Research Center of Big Data for Sustainable Development Goals (No. CBAS2022DF006). We thank the anonymous reviewers for their valuable comments and suggestions.

Author contributions

Q.X., A.H., and A.L. designed the study. Q.X., C.E.M., and C.C.H. collected the data and performed the data analysis. Q.X. wrote the first draft of the manuscript. All authors contributed to the discussion, writing, editing, and revising of the manuscript.

References

ABARES, 2022. Australian Bureau of Agriculture and Resources Economics and Science (ABARES), https://www.agriculture.gov.au/abares/products/insights/snapshot-of-australian-agriculture-2022. https://doi.org/https://www.agriculture.gov.au/abares/products/insights/snapshot-of-australian-agriculture-2022.

Arndt, S., 2013. Wombat State Forest OzFlux-tower site OzFlux: Australian and New Zealand Flux Research and Monitoring hdl: 102.100.100/14237.

Baldocchi, D., Falge, E., Gu, L., Olson, R., Hollinger, D., Running, S., Anthoni, P., Bernhofer, C., Davis, K., Evans, R., 2001. FLUXNET: A new tool to study the temporal and spatial variability of ecosystem-scale carbon dioxide, water vapor, and energy flux densities. Bull. Am. Meteorol. Soc. 82, 2415–2434.

Barr, A.G., Richardson, A.D., Hollinger, D.Y., Papale, D., Arain, M.A., Black, T.A., Bohrer, G., Dragoni, D., Fischer, M.L., Gu, L., 2013. Use of change-point detection for friction–velocity threshold evaluation in eddy-covariance studies. Agric. For. Meteorol. 171, 31–45.

Baumann, M., Ozdogan, M., Richardson, A.D., Radeloff, V.C., 2017. Phenology from Landsat when data is scarce: Using MODIS and Dynamic Time-Warping to combine multi-year Landsat imagery to derive annual phenology curves. Int. J. Appl. Earth Obs. Geoinf. 54, 72–83. https://doi.org/10.1016/j.jag.2016.09.005.

Beringer, J., Moore, C.E., Cleverly, J., Campbell, D.I., Cleugh, H., Kauwe, M.G.D., Kirschbaum, M.U.F., Griebel, A., Grover, S., Huete, A., Hutley, L.B., Laubach, J., Niel, T.V., Arndt, S.K., Bennett, A.C., Cernusak, L.A., Eamus, D., Ewenz, C.M., Goodrich, J.P., Hinko-, M.J.N., Isaac, N.P., Hobeichi, S., Knauer, J., Koerber, G.R., Liddell, M., Ma, X., Macfarlane, C., Mchugh, I.D., Medlyn, B.E., Meyer, W.S., Norton, A.J., Owens, J., Pitman, A., Pendall, E., Prober, S.M., Ray, R.L., Silberstein, R.P., Teckentrup, L., Thompson, S.E., Ukkola, A.M., Ying-, A.W., Wang, P., Wardlaw, T.J., 2022. Bridge to the future: Important lessons from 20 years of ecosystem observations made by the OzFlux network. Glob. Chang. Biol. 1–26 https://doi.org/10.1111/gcb.16141.

Beringer, 2013a. Yanco JAXA OzFlux tower site OzFlux: Australian and New Zealand Flux Research and Monitoring hdl: 102.100.100/14235.

Beringer, 2013b. Sturt Plains OzFlux tower site OzFlux: Australian and New Zealand Flux Research and Monitoring hdl: 102.100.100/14230.

Beringer, 2013c. Dry River OzFlux tower site OzFlux: Australian and New Zealand flux research and monitoring hdl:102.100.100/14229.

Beringer, 2013d. Howard Springs OzFlux tower site OzFlux: Australian and New Zealand Flux Research and Monitoring hdl: 102.100.100/14234.

Beringer, 2013e. Daly Uncleared OzFlux site OzFlux: Australian and New Zealand flux research and monitoring hdl: 102.100.100/14239.

Bolton, D.K., Gray, J.M., Melaas, E.K., Moon, M., Eklundh, L., Friedl, M.A., 2020. Continental-scale land surface phenology from harmonized Landsat 8 and Sentinel-2 imagery. Remote Sens. Environ. 240, 111685 https://doi.org/10.1016/J.RSE.2020.111685.

Bornez, K., Descals, A., Verger, A., Peñuelas, J., 2020. Land surface phenology from VEGETATION and PROBA-V data. Assessment over deciduous forests. Int. J. Appl. Earth Obs. Geoinf. 84, 101974.

Broich, M., Huete, A., Tulbure, M.G., Ma, X., Xin, Q., Paget, M., Restrepo-Coupe, N., Davies, K., Devadas, R., Held, A., 2014. Land surface phenological response to decadal climate variability across Australia using satellite remote sensing. Biogeosciences 11, 5181–5198. https://doi.org/10.5194/bg-11-5181-2014.

Broich, M., Huete, A., Paget, M., Ma, X., Tulbure, M., Coupe, N.R., Evans, B., Beringer, J., Devadas, R., Davies, K., Held, A., 2015. A spatially explicit land surface phenology data product for science, monitoring and natural resources management applications. Environ. Model. Softw. 64, 191–204. https://doi.org/10.1016/j.envsoft.2014.11.017.

Brown, M.E., de Beurs, K., Vrieling, A., 2010. The response of African land surface phenology to large scale climate oscillations. Remote Sens. Environ. 114, 2286–2296.

Bureau of Meteorology, CSIRO, 2020. State of the climate 2020. State of the climate.

Cao, R., Chen, J., Shen, M., Tang, Y., 2015. An improved logistic method for detecting spring vegetation phenology in grasslands from MODIS EVI time-series data. Agric. For. Meteorol. 200, 9–20. https://doi.org/10.1016/j.agrformet.2014.09.009.

Chapin, F.S., Woodwell, G.M., Randerson, J.T., Rastetter, E.B., Lovett, G.M., Baldocchi, D.D., Clark, D.A., Harmon, M.E., Schimel, D.S., Valentini, R., 2006. Reconciling carbon-cycle concepts, terminology, and methods. Ecosystems 9, 1041–1050.

Cleverly, J., Eamus, D., Luo, Q., Coupe, N.R., Kljun, N., Ma, X., Ewenz, C., Li, L., Yu, Q., Huete, A., 2016a. The importance of interacting climate modes on Australia's contribution to global carbon cycle extremes. Sci. Rep. 6, 1–10.

Cleverly, J., Eamus, D., Restrepo Coupe, N., Chen, C., Maes, W., Li, L., Faux, R., Santini, N.S., Rumman, R., Yu, Q., Huete, A., 2016b. Soil moisture controls on phenology and productivity in a semi-arid critical zone. Sci. Total Environ. 568, 1227–1237. https://doi.org/10.1016/j.scitotenv.2016.05.142.

Cleverly, J., 2011. Alice Springs Mulga OzFlux site OzFlux: Australian and New Zealand Flux Research and Monitoring hdl: 102.100.100/14217.

Delbart, N., Beaubien, E., Kergoat, L., Le Toan, T., 2015. Comparing land surface phenology with leafing and flowering observations from the PlantWatch citizen network. Remote Sens. Environ. 160, 273–280.

Didan, K., Munoz, A.B., Solano, R., Huete, A., 2015. MODIS vegetation index user's guide (MOD13 series). University of Arizona, Vegetation Index and Phenology Lab.

Dougherty, R.L., Edelman, A.S., Hyman, J.M., 1989. Nonnegativity-, monotonicity-, or convexity-preserving cubic and quintic Hermite interpolation. Math. Comput. 52, 471–494.

Eamus, D., Huete, A., Cleverly, J., Nolan, R.H., Ma, X., Tarin, T., Santini, N.S., 2016. Mulga, a major tropical dry open forest of Australia: recent insights to carbon and water fluxes. Environ. Res. Lett. 11 https://doi.org/10.1088/1748-9326/11/12/125011.

Gray, J., Sulla-Menashe, D., Friedl, M.A., 2019. User Guide to Collection 6 MODIS Land Cover Dynamics (MCD12Q2) Product. User Guide 6, 1–8.

V. Haverd M.R. Raupach P.R. Briggs Canadell., J.G., Davis, S.J., Law, R.M., Meyer, C.P., Peters, G.P., Pickett-Heaps, C., Sherman, B., The Australian terrestrial carbon budget Biogeosciences 10 2013 851 869 10.5194/bg-10-851-2013.

Helman, D., 2017. Land surface phenology: What do we really "see" from space? Sci. Total Environ. https://doi.org/10.1016/j.scitotenv.2017.07.237.

Henebry, G.M., de Beurs, K.M., 2013. Remote sensing of land surface phenology: A prospectus. An Integrative Environmental Science. Springer, Phenology, pp. 385–411.

Hersbach, H., Bell, B., Berrisford, P., Hirahara, S., Horányi, A., Muñoz-Sabater, J., Nicolas, J., Peubey, C., Radu, R., Schepers, D., 2017. Complete ERA5 from 1979: Fifth generation of ECMWF atmospheric reanalyses of the global climate. Copernicus Climate Change Service (C3S) Data Store (CDS), ECMWF.

Hsu, K., Gupta, H.V., Gao, X., Sorooshian, S., Imam, B., 2002. Self-organizing linear output map (SOLO): An artificial neural network suitable for hydrologic modeling and analysis. Water Resour. Res. 38, 31–38.

Huete, A., Didan, K., Miura, T., Rodriguez, E.P., Gao, X., Ferreira, L.G., 2002. Overview of the radiometric and biophysical performance of the MODIS vegetation indices. Remote Sens. Environ. 83, 195–213.

Huete, A.R., Didan, K., Shimabukuro, Y.E., Ratana, P., Saleska, S.R., Hutyra, L.R., Yang, W., Nemani, R.R., Myneni, R., 2006. Amazon rainforests green-up with sunlight in dry season. Geophys. Res. Lett. 33.

Hughes, L., 2011. Climate change and Australia: Key vulnerable regions. Reg. Environ. Chang. 11, 189–195. https://doi.org/10.1007/s10113-010-0158-9.

Isaac, P., Cleverly, J., McHugh, I., Van Gorsel, E., Ewenz, C., Beringer, J., 2017. OzFlux data: Network integration from collection to curation. Biogeosciences 14, 2903–2928. https://doi.org/10.5194/bg-14-2903-2017.

Ji, Z., Pan, Y., Zhu, X., Zhang, D., Wang, J., 2022. A generalized model to predict large-scale crop yields integrating satellite-based vegetation index time series and phenology metrics. Ecol. Ind. 137, 108759.

Kato, A., Carlson, K.M., Miura, T., 2021. Assessing the inter-annual variability of vegetation phenological events observed from satellite vegetation index time series in dryland sites. Ecol. Ind. 130, 108042.

Keenan, T.F., Gray, J., Friedl, M.A., Toomey, M., Bohrer, G., Hollinger, D.Y., Munger, J. W., O'Keefe, J., Schmid, H.P., Wing, I.S., Yang, B., Richardson, A.D., 2014. Net carbon uptake has increased through warming-induced changes in temperate forest phenology. Nat. Clim. Chang. 4, 598–604. https://doi.org/10.1038/nclimate2253.

King, A.D., Pitman, A.J., Henley, B.J., Ukkola, A.M., Brown, J.R., 2020. The role of climate variability in Australian drought. Nat. Clim. Chang. 10, 177–179.

Li, F., Song, G., Liujun, Z., Yanan, Z., Di, L., 2017. Urban vegetation phenology analysis using high spatio-temporal NDVI time series. Urban For. Urban Green. 25, 43–57.

Linderholm, H.W., 2006. Growing season changes in the last century. Agric. For. Meteorol. 137, 1–14.

Lloyd, D., 1990. A phenological classification of terrestrial vegetation cover using shortwave vegetation index imagery. Int. J. Remote Sens. 11, 2269–2279. https://doi.org/10.1080/01431169008955174.

Lloyd, J., Taylor, J.A., 1994. On the temperature dependence of soil respiration. Funct. Ecol. 315–323.

Loveland, T.R., Reed, B.C., Brown, J.F., Ohlen, D.O., Zhu, Z., Yang, L., Merchant, J.W., 2000. Development of a global land cover characteristics database and IGBP DISCover from 1 km AVHRR data. Int. J. Remote Sens. 21, 1303–1330.

Lymburner, L., Tan, P., Mueller, N., Thackway, R., Lewis, A., Thankappan, M., Randall, L., Islam, A., Senarath, U., 2011. The National Dynamic Land Cover Dataset. Geoscience Australia, Symonston, Australia, p. 10.

Ma, X., Huete, A., Yu, Q., Coupe, N.R., Davies, K., Broich, M., Ratana, P., Beringer, J., Hutley, L.B., Cleverly, J., Boulain, N., Eamus, D., 2013. Spatial patterns and temporal dynamics in savanna vegetation phenology across the North Australian Tropical Transect. Remote Sens. Environ. 139, 97–115. https://doi.org/10.1016/j.rse.2013.07.030.

Ma, X., Huete, A., Cleverly, J., Eamus, D., Chevallier, F., Joiner, J., Poulter, B., Zhang, Y., Guanter, L., Meyer, W., 2016. Drought rapidly diminishes the large net CO2 uptake in 2011 over semi-arid Australia. Sci. Rep. 6, 1–9.

Ma, X., Zhu, X., Xie, Q., Jin, J., Zhou, Y., Luo, Y., Liu, Y., Tian, J., Zhao, Y., 2022. Monitoring nature's calendar from space: Emerging topics in land surface phenology and associated opportunities for science applications. Glob. Chang. Biol. 7186–7204 https://doi.org/10.1111/gcb.16436.

MacFarlane, C., 2013. Great Western Woodlands OzFlux: Australian and New Zealand Flux Research and Monitoring hdl: 102.100.100/14226.

Miller, M.E., Belote, R.T., Bowker, M.A., Garman, S.L., 2011. Alternative states of a semiarid grassland ecosystem: implications for ecosystem services. Ecosphere 2, 1–18.

Moore, C.E., Brown, T., Keenan, T.F., Duursma, R.A., Van Dijk, A.I.J.M., Beringer, J., Culvenor, D., Evans, B., Huete, A., Hutley, L.B., Maier, S., Restrepo-Coupe, N., Sonnentag, O., Specht, A., Taylor, J.R., Van Gorsel, E., Liddell, M.J., 2016. Reviews and syntheses: Australian vegetation phenology: New insights from satellite remote sensing and digital repeat photography. Biogeosciences 13, 5085–5102. https://doi.org/10.5194/bg-13-5085-2016.

Morton, S.R., Smith, D.M.S., Dickman, C.R., Dunkerley, D.L., Friedel, M.H., McAllister, R. R.J., Reid, J.R.W., Roshier, D.A., Smith, M.A., Walsh, F.J., 2011. A fresh framework for the ecology of arid Australia. J. Arid Environ. 75, 313–329.

Myneni, R.B., Keeling, C.D., Tucker, C.J., Asrar, G., Nemani, R.R., 1997. Increased plant growth in the northern high latitudes from 1981 to 1991. Nature 386, 698.

Nolan, R.H., Foster, B., Griebel, A., Choat, B., Medlyn, B.E., Yebra, M., Younes, N., Boer, M.M., 2022. Drought-related leaf functional traits control spatial and temporal dynamics of live fuel moisture content. Agric. For. Meteorol. 319, 108941.

Pendall, E., 2015. Cumberland Plain OzFlux Tower Site OzFlux: Australian and New Zealand Flux Research and Monitoring hdl: 102.100.100/25164.

Peng, D., Wu, C., Li, C., Zhang, X., Liu, Z., Ye, H., Luo, S., Liu, X., Hu, Y., Fang, B., 2017a. Spring green-up phenology products derived from MODIS NDVI and EVI: Intercomparison, interpretation and validation using National Phenology Network and AmeriFlux observations. Ecol. Ind. 77, 323–336. https://doi.org/10.1016/j.ecolind.2017.02.024.

Peng, D., Zhang, X., Wu, C., Huang, W., Gonsamo, A., Huete, A.R., Didan, K., Tan, B., Liu, X., Zhang, B., 2017b. Intercomparison and evaluation of spring phenology products using National Phenology Network and AmeriFlux observations in the contiguous United States. Agric. For. Meteorol. 242, 33–46. https://doi.org/10.1016/j.agrformet.2017.04.009.

Peng, D., Wang, Y., Xian, G., Huete, A.R., Huang, W., Shen, M., Wang, F., Yu, L., Liu, L., Xie, Q., Liu, L., Zhang, X., 2021. Investigation of land surface phenology detections in shrublands using multiple scale satellite data. Remote Sens. Environ. 252 https://doi.org/10.1016/j.rse.2020.112133.

Peñuelas, J., Filella, I., 2009. Phenology feedbacks on climate change. Science 324, 887–888.

Phillips, A., 2015. Warra OzFlux tower site OzFlux: Australian and New Zealand Flux Research and Monitoring hdl: 102.100.100/22566.

Piao, S., Liu, Q., Chen, A., Janssens, I.A., Fu, Y., Dai, J., Liu, L., Lian, X., Shen, M., Zhu, X., 2019. Plant phenology and global climate change: Current progresses and challenges. Glob. Chang. Biol. 25, 1922–1940. https://doi.org/10.1111/gcb.14619.

Pörtner, H.-O., Roberts, D.C., Tignor, M., E.S. Poloczanska, K.M., Alegría, A., M. Craig, S. L., S. Löschke, V. Möller, A. Okem, B.R., 2022. Climate Change 2022: Impacts, Adaptation, and Vulnerability. Contribution of Working Group II to the Sixth Assessment Report of the Intergovernmental Panel on Climate Change.

Poulter, B., Frank, D., Ciais, P., Myneni, R.B., Andela, N., Bi, J., Broquet, G., Canadell, J. G., Chevallier, F., Liu, Y.Y., Running, S.W., Sitch, S., Van Der Werf, G.R., 2014. Contribution of semi-arid ecosystems to interannual variability of the global carbon cycle. Nature 509, 600–603. https://doi.org/10.1038/nature13376.

Puma, M.J., Koster, R.D., Cook, B.I., 2013. Phenological versus meteorological controls on land-atmosphere water and carbon fluxes. J. Geophys. Res. Biogeo. 118, 14–29.

Ren, S., Li, Y., Peichl, M., 2020. Diverse effects of climate at different times on grassland phenology in mid-latitude of the Northern Hemisphere. Ecol. Ind. 113, 106260.

Restrepo-Coupe, N., Huete, A., Davies, K., Cleverly, J., Beringer, J., Eamus, D., Van Gorsel, E., Hutley, L.B., Meyer, W.S., 2016. MODIS vegetation products as proxies of photosynthetic potential along a gradient of meteorologically and biologically driven ecosystem productivity. Biogeosciences 13, 5587–5608. https://doi.org/10.5194/bg-13-5587-2016.

Richardson, A.D., Anderson, R.S., Arain, M.A., Barr, A.G., Bohrer, G., Chen, G., Chen, J. M., Ciais, P., Davis, K.J., Desai, A.R., 2012. Terrestrial biosphere models need better representation of vegetation phenology: results from the North American Carbon Program Site Synthesis. Glob. Chang. Biol. 18, 566–584.

Richardson, A.D., Keenan, T.F., Migliavacca, M., Ryu, Y., Sonnentag, O., Toomey, M., 2013. Climate change, phenology, and phenological control of vegetation feedbacks to the climate system. Agric. For. Meteorol. 169, 156–173. https://doi.org/10.1016/j.agrformet.2012.09.012.

Richardson, A.D., Hufkens, K., Milliman, T., Aubrecht, D.M., Chen, M., Gray, J.M., Johnston, M.R., Keenan, T.F., Klosterman, S.T., Kosmala, M., Melaas, E.K., Friedl, M. A., Frolking, S., 2018. Tracking vegetation phenology across diverse North American biomes using PhenoCam imagery. Sci. Data 5, 1–24. https://doi.org/10.1038/sdata.2018.28.

Rowlings, D., 2011. Samford Ecological Research Facility OzFlux tower site OzFlux: Australian and New Zealand Flux Research and Monitoring hdl: 102.100.100/14219.

Savitzky, A., Golay, M.J.E., 1964. Smoothing and differentiation of data by simplified least squares procedures. Anal. Chem. 36, 1627–1639.

Shen, M., Piao, S., Cong, N., Zhang, G., Jassens, I.A., 2015. Precipitation impacts on vegetation spring phenology on the Tibetan Plateau. Glob. Chang. Biol. 21, 3647–3656. https://doi.org/10.1111/gcb.12961.
Silberstein, R., 2015. Gingin OzFlux: Australian and New Zealand Flux Research and Monitoring hdl: 102.100.100/22677.
Stern, H., De Hoedt, G., Ernst, J., 2000. Objective classification of Australian climates. Aust. Met. Mag. 49, 87–96.
Sulla-Menashe, D., Friedl, M.A., 2018. User guide to collection 6 MODIS land cover (MCD12Q1 and MCD12C1) product. USGS: Reston, VA, USA 1–18.
Tech, C., 2013. Calperum Chowilla OzFlux tower site OzFlux: Australian and New Zealand Flux Research and Monitoring hdl: 102.100.100/14236.
Thompson, J.A., Paull, D.J., 2017. Assessing spatial and temporal patterns in land surface phenology for the Australian Alps (2000–2014). Remote Sens. Environ. 199, 1–13. https://doi.org/10.1016/j.rse.2017.06.032.
Tong, X., Tian, F., Brandt, M., Liu, Y., Zhang, W., Fensholt, R., 2019. Trends of land surface phenology derived from passive microwave and optical remote sensing systems and associated drivers across the dry tropics 1992–2012. Remote Sens. Environ. 232, 111307 https://doi.org/10.1016/j.rse.2019.111307.
Walther, S., Voigt, M., Thum, T., Gonsamo, A., Zhang, Y., Köhler, P., Jung, M., Varlagin, A., Guanter, L., 2016. Satellite chlorophyll fluorescence measurements reveal large-scale decoupling of photosynthesis and greenness dynamics in boreal evergreen forests. Glob. Chang. Biol. 22, 2979–2996. https://doi.org/10.1111/gcb.13200.
Wang, C., Beringer, J., Hutley, L.B., Cleverly, J., Li, J., Liu, Q., Sun, Y., 2019. Phenology Dynamics of Dryland Ecosystems Along the North Australian Tropical Transect Revealed by Satellite Solar-Induced Chlorophyll Fluorescence. Geophys. Res. Lett. 46, 5294–5302. https://doi.org/10.1029/2019GL082716.
Wang, S., Zhang, L., Huang, C., Qiao, N., 2017. An NDVI-Based Vegetation Phenology Is Improved to be More Consistent with Photosynthesis Dynamics through Applying a Light Use Efficiency Model over Boreal High-Latitude Forests. Remote Sens. (Basel) 9. https://doi.org/10.3390/rs9070695.
White, M.A., Thornton, P.E., Running, S.W., 1997. A continental phenology model for monitoring vegetation responses to interannual climatic variability. Global Biogeochem. Cycles 11, 217–234. https://doi.org/10.1029/97gb00330.
White, M.A., de Beurs, K.M., Didan, K., Inouye, D.W., Richardson, A.D., Jensen, O.P., O'keefe, J., Zhang, G., Nemani, R.R., van Leeuwen, W.J.D., 2009. Intercomparison, interpretation, and assessment of spring phenology in North America estimated from remote sensing for 1982–2006. Glob. Chang. Biol. 15, 2335–2359.
Woodgate, W., 2013. Tumbarumba OzFlux tower site OzFlux: Australian and New Zealand Flux Research and Monitoring hdl: 102.100.100/14241.
Wu, C., Wang, J., Ciais, P., Peñuelas, J., Zhang, X., Sonnentag, O., Tian, F., Wang, X., Wang, H., Liu, R., Fu, Y.H., Ge, Q., 2021. Widespread decline in winds delayed autumn foliar senescence over high latitudes. Proceedings of the National Academy of Sciences 118, e2015821118. https://doi.org/10.1073/pnas.2015821118.
Wu, C., Hou, X., Peng, D., Gonsamo, A., Xu, S., 2016. Land surface phenology of China's temperate ecosystems over 1999–2013: Spatial-temporal patterns, interaction effects, covariation with climate and implications for productivity. Agric. For. Meteorol. 216, 177–187. https://doi.org/10.1016/j.agrformet.2015.10.015.
Xie, Q., Cleverly, J., Moore, C.E., Ding, Y., Hall, C.C., Ma, X., Brown, L.A., Wang, C., Beringer, J., Prober, S.M., Macfarlane, C., Meyer, W.S., Yin, G., Huete, A., 2022a. Land surface phenology retrievals for arid and semi-arid ecosystems. ISPRS J. Photogramm. Remote Sens. 185, 129–145. https://doi.org/10.1016/j.isprsjprs.2022.01.017.
Xie, Q., Huete, A., Hall, C.C., Medlyn, B.E., Power, S.A., Davies, J.M., Medek, D.E., Beggs, P.J., 2022b. Satellite-observed shifts in C3 / C4 abundance in Australian grasslands are associated with rainfall patterns. Remote Sens. Environ. 273, 112983 https://doi.org/10.1016/j.rse.2022.112983.
Xin, Q., Broich, M., Suyker, A.E., Yu, L., Gong, P., 2015. Multi-scale evaluation of light use efficiency in MODIS gross primary productivity for croplands in the Midwestern United States. Agric. For. Meteorol. 201, 111–119.
Xu, X., Riley, W.J., Koven, C.D., Jia, G., 2019. Heterogeneous spring phenology shifts affected by climate: supportive evidence from two remotely sensed vegetation indices. Environ. Res. Commun. 1, 091004 https://doi.org/10.1088/2515-7620/ab3d79.
Zhang, X., Friedl, M.A., Schaaf, C.B., Strahler, A.H., Hodges, J.C., Gao, F., Reed, B.C., Huete, A., 2003. Monitoring vegetation phenology using MODIS. Remote Sens. Environ. 84, 471–475.
Zhang, X., Friedl, M.A., Schaaf, C.B., 2006. Global vegetation phenology from Moderate Resolution Imaging Spectroradiometer (MODIS): Evaluation of global patterns and comparison with in situ measurements. J. Geophys. Res. Biogeosci. 111.
Zhang, Y., Lim, S., Sharples, J.J., 2017. Wildfire occurrence patterns in ecoregions of New South Wales and Australian Capital Territory, Australia. Nat. Hazards 87, 415–435. https://doi.org/10.1007/s11069-017-2770-1.
Zhang, X., Liu, L., Liu, Y., Jayavelu, S., Wang, J., Moon, M., Henebry, G.M., Friedl, M.A., Schaaf, C.B., 2018. Generation and evaluation of the VIIRS land surface phenology product. Remote Sens. Environ. 216, 212–229.
Zhang, X., Liu, L., Henebry, G.M., 2019. Impacts of land cover and land use change on long-term trend of land surface phenology: A case study in agricultural ecosystems. Environ. Res. Lett. 14 https://doi.org/10.1088/1748-9326/ab04d2.
Zhao, D., Hou, Y., Zhang, Z., Wu, Y., Zhang, X., Wu, L., Zhu, X., Zhang, Y., 2022. Temporal resolution of vegetation indices and solar-induced chlorophyll fluorescence data affects the accuracy of vegetation phenology estimation: A study using in-situ measurements. Ecol. Ind. 136, 108673.
Zhou, L., Zhou, W., Chen, J., Xu, X., Wang, Y., Zhuang, J., Chi, Y., 2022. Land surface phenology detections from multi-source remote sensing indices capturing canopy photosynthesis phenology across major land cover types in the Northern Hemisphere. Ecol. Ind. 135, 108579.